Cloud Curves of Polystyrene or Poly(methyl methacrylate) or Poly(styrene-*co*-methyl methacrylate) in Cyclohexanol Determined with a Thermo-Optical Apparatus

V. García Sakai,† J. S. Higgins, and J. P. M. Trusler*

Department of Chemical Engineering, Imperial College London, South Kensington Campus, London SW7 2AZ, U.K.

A turbidimeter has been developed for rapid, automatic, and precise cloud-curve measurements in polymer solutions. The apparatus combines five sample cells in a single unit and so permits five different compositions to be studied in a single heating or cooling ramp, leading to rapid characterization of the cloud curve. The apparatus can be used in the temperature range 293 to 523 K at pressures up to approximately 3 MPa. The instrument was tested in measurements on the system PS + cyclohexane, where PS is polystyrene, and subsequently used to measure the cloud curves of PMMA + cyclohexanol and PS-*b*-MMA + cyclohexanol, where PMMA is poly(methyl methacrylate) and PS-*b*-MMA is a 50:50 block copolymer formed from styrene and methyl methacrylate. The effect of polymer molar mass was studied. All systems showed upper critical solution temperatures.

Introduction

In this paper, we describe a simple thermo-optical apparatus that permits rapid measurement of the cloud-point curves of binary polymer solutions, and we present results for several industrially important polymers dissolved in cyclohexanol. The motivation for this research[1] was 2-fold: first, experimental techniques were required for measuring cloud curves that were as reliable as visual observation but automated and more rapid; second, there were continuing industrial needs for reliable data and models on polymer solution phase behavior. The polymers considered in this study are among the most important industrially, and their phase behavior in common nonpolar solvents is well-known. However, there are fewer data available for these polymers in polar or associating solvents. Accordingly, we chose cyclohexanol as the solvent in this study. The results will be particularly challenging for thermodynamic models as they combine a polymer having polar functional groups with a polar and associating solvent.

Previous Studies. Liquid−liquid equilibria (LLE) of polymer solutions have been studied extensively, and collections of data are available in the literature. For example, Hao et al.[2] presented a compilation of LLE data, activities, and solubilities for polymer solutions. Other useful sources include High and Danner[3] and Wohlfarth.[4]

Before describing the instrumentation developed in this work, we first review briefly the most common types of LLE observed in binary polymer solutions. Such data are usually represented on either isobaric or orthobaric temperature−composition ($T-w$) diagrams, where w denotes the mass fraction of polymer. The most commonly observed $T-w$ diagram for polymer solutions exhibits a single binodal curve with an upper critical solution temperature (UCST) below which the system separates into two co-exisitng phases. Examples include polyethylene (PE) + ethylene,[5] polyisobutylene (PIB) + diisobutyl ketone,[6] and poly-α-methylstyrene + methyl cyclohexane.[7] On the other hand, lower critical solution temperature (LCST) behavior is observed for a number of common systems such as PE[8] and PIB[9] in various *n*-alkane solvents as well as in polystyrene (PS) + benzene and PS + methyl elthyl ketone.[10] Both UCST and LCST behavior have been found for PS + cyclohexane.[10] In this case, the LCST is above the UCST, and the system is miscible in all proportions at intermediate temperatures. This type of $T-w$ diagram has also been observed in PS + methyl acetate[11] and PS + ethyl formate[12] and in other systems such as cellulose acetate + acetone[13] and poly(styrene-*co*-α-methyl styrene) + cyclohexane.[14] Closed-loop $T-w$ diagrams are formed when the UCST is above than the LCST. This is observed in some highly polar systems such as poly(ethylene glycol) (PEG) + water[15] and poly(butyl methyl acrylate) or poly(styrene-*co*-butyl methyl acrylate) + methyl ethyl ketone.[16] Finally we recall that $T-w$ diagrams exist in which there is a miscibility gap that first narrows and then widens again with increasing temperature. This type of "hour-glass" diagram has been observed for PS + acetone and some PS + diethyl ether systems.[15] A similar set of elementary isothermal $p-w$ diagrams exist with upper and lower critical solution pressures.

Polymer solution phase diagrams have a number of common characteristics that distinguish them from binary mixtures of low molar mass components. Most notably, the coexistence curves are typically highly asymmetric with respect to composition and also flat in a wide composition range around the critical point. In addition, the phase diagram is quantitatively, and some times qualitatively, dependent upon the molar mass of the polymer. Most of the common $T-w$ diagrams can be studied effectively along isopleths, although, for example, it is necessary to vary composition in order to obtain parts of the closed-loop and hour-glass diagrams.

Experimental Methods. The simplest experimental method for determining the binodal curves of polymer solutions is visualization of the sample during a temperature ramp operation that crosses this curve. Typically, a mixture of known overall composition is sealed in a glass cell and placed in a thermostat bath fitted with an observation window. The bath temperature

* Corresponding author. E-mail: m.trusler@imperial.ac.uk.
† Present address: NIST Center for Neutron Research, Gaithersburg, MD 20899, and Department of Materials Science and Engineering, University of Maryland, College Park, MD 20742.

10.1021/je0504865 CCC: $33.50
Published on Web 01/27/2006

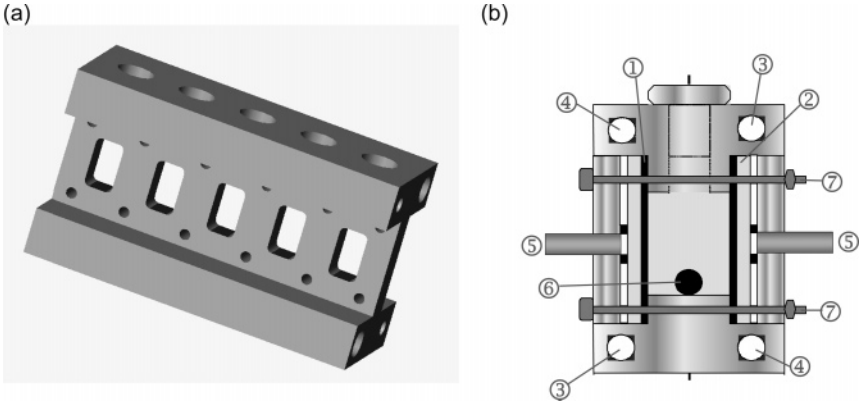

Figure 1. Cell block: panel a, isometric projection; panel b, cross-sectional sketch. 1, Viton gasket; 2, borosilicate glass windows; 3, cartridge heaters; 4, heat exchanger tube; 5, optical path; 6, stainless steel ball; 7, assembly bolts.

is then ramped up or down slowly, and the transition from homogeneous to heterogeneous phase behavior can be observed as a cloud-point. If the cells are fitted with a stirring device or agitated by other means, then the experiment can be repeated in the reverse direction (heterogeneous to homogeneous transition) and the results compared. The method is manual, slow, and somewhat subjective but nevertheless reliable. The cloud curves of poly(α-methyl styrene) + methyl cyclohexane were measured in this way by Pruessner et al.,[7] while Saeki et al.[10,11] measured cloud curves for solutions of PS in a number of different solvents at mass fractions of polymer of up to 0.25.

Sealed cells containing only polymer and solvent, with a small vapor space present, lead to orthobaric conditions; hence, measured points on the cloud curve correspond to liquid−liquid−vapor equilibrium (LLVE) rather than isobaric LLE. Isobaric LLE may be observed visually in a windowed autoclave fitted with a means of controlling pressure. The same arrangement may be used to study isothermal LLE (leading to a $p-w$ diagram), and in either mode, high pressures may be imposed. For example, Meilchen et al.[17] used a variable-volume autoclave for measurements at pressures up to 200 MPa and reported cloud curve data for solutions of poly(ethylene-*co*-methacrylate) in either propane or chlorodifluoromethane.

The subjective nature of visual observation may be eliminated by measuring the turbidity of the sample or the light scattered from it or both with the aid of photoelectric devices. Crossing the phase boundary from homogeneous to heterogeneous states results in a sharp increase in both turbidity and light scattering. A He−Ne laser beam is typically used in light scattering experiments, although an incandescent or light-emitting-diode source may be used for turbidity measurements. Again, the sample may be contained within a sealed glass cell or a windowed autoclave; the latter arrangement has been used to measure the isothermal LLE of PS + cyclohexane and PS + methyl cyclohexane by light scattering technique.[18,19]

Observations of cloud-points in dynamic (heating or cooling) experiments can be subject to systematic errors arising from kinetic effects. For example, Szydlowski and van Hook[18] have discussed the possible effect of quenching rates on observed cloud-point temperatures. However, Bae et al.[20] measured cloud-points by thermo-optical analysis for monodisperse PS (M_w = 100 kg·mol^{-1}) in cyclohexane at three different cooling rates (0.1, 0.3, and 0.5 K·min^{-1}) and found the same results in each case. In this work, we favored the simplicity of a turbidity measurement over light scattering techniques, but we adopted an automated and objective methodology.

Experimental Section

Apparatus. The turbidimeter was designed to measure cloud-points at temperatures ranging from 293 K to 523 K and to withstand pressures up to 3 MPa. The design incorporated five sample cells in a single metal block, thereby enabling simultaneous measurements on five compositions and more rapid characterization of the cloud curve in $T-w$ space.

The body of the apparatus, illustrated in Figure 1, consisted of an aluminum I-piece of length 95 mm, width 35 mm, and height 54 mm. Through this were bored five rectangular holes that formed cells of volume approximately 0.9 mL each. A filling port was provided in the top of each cell, and this was plugged by a screw cap and sealed with a viton O-ring. The faces of the cells were closed by 3 mm thick borosilicate glass windows sealed by a viton gasket of thickness 1.5 mm. The windows were retained by aluminum plates (one on each side of the cell block) and a set of 12 bolts. To achieve sufficient local compression of the viton gasket, the sealing surfaces of the main body were machined with a pattern of troughs (not shown in Figure 1), leaving a small raised surface over which the seal was effected.

The cell block was heated by means of two 50 W cartridge heaters located in holes running along the length of the body. Two more tubular passages passed along the length of the body, and these served as heat exchangers for cooling. Chilled nitrogen gas was passed through these heat exchangers when cooling was required. A pair of PT100 platinum resistance thermometers were located in close-fitting wells in the bottom of the cell block. One of these was used as the control sensor, and the other was used for measurement purposes. The temperature of the cell block was controlled by a precision PID process controller capable of executing programmed temperature ramps. The measurement thermometer was calibrated by comparison with a standard platinum resistance thermometer that had itself been calibrated on ITS-90 at the UK National Physical Laboratory. The estimated expanded uncertainty ($k = 2$) of the temperature measurements was 0.03 K.

Light was generated by a set of five light-emitting signal diodes with SMA fitings driven at a constant current of 47 mA under which conditions, according to the manufacturers data sheet, they emitted about 50 μW of red light with a peak emission wavelength of 660 nm. The light was passed along a set of 250 μm diameter optical fibers, each terminated by an adaptor screwed into holes that passed through the aluminum plate used to retain the windows. These adaptors each contained a plano-convex lens that produced a parallel light beam of diameter 4 mm. After passing through the sample space between

Table 1. Characteristics of the Polymers Used in This Work[a]

polymer	M_w/(kg·mol^{-1})	M_w/M_n	w_{PS}
PS 4	4.215	1.07	
PS 79	78.8	1.12	
PS 286	286	2.2	
PS 850	849	1.45	
PMMA 68	68.0	1.03	
PMMA 280	280	1.06	
PMMA 992	992.2	1.06	
PS-*b*-MMA 59	58.5	1.06	0.487

[a] M_w,weight-average molar mass; M_n, number-average molar mass; and w_{PS}, weight fraction of polystyrene for the copolymer.

the windows, the transmitted light was gathered by a similar adaptor and transmitted through another optical fiber to an SMA photodetector. The dc voltages generated by the photodetector circuits were measured with a data acquisition unit, fitted with a 20-channel multiplexer, and logged by a computer. The platinum resistance thermometer was also connected to the data acquisition system, and it was therefore possible to monitor temperature and turbidity in each cell almost continuously during temperature ramping.

The dark signals from the photodetector circuits were measured with the light sources turned off, and the combined effects of noise and drift were found to be bounded by ± 1 mV. Next, the LEDs were then turned on, and the signal through the empty cells was monitored over a period of time. It was found that a warm-up period of approximately 30 min was required, after which the signal measured at the photodetector was stable to about ± 2 mV.

To minimize temperature gradients and reduce heat losses, the cell block was insulated by 25 mm thick expanded silicone sponge sheets, and the entire assembly was enclosed in an aluminum box. Holes in the insulation and outer box were provided for the optical channels, thermometer lead wires, and flexible stainless steel tubes connected to the heat exchanger. The entire apparatus was mounted on a motor drive that permitted it to be rotated back and forth around its major axis with an amplitude of up to ± 180°. Furthermore, each cell contained a 4 mm diameter stainless steel ball that, during rocking, served to enhance agitation. In their rest positions at the bottom of the cell, these balls were just outside the optical system's field of view.

Materials. Polydisperse polystyrene of molar mass 286 kg·mol^{-1} was characterized using gel permeation chromatography by RAPRA Technology Ltd. Monodisperse samples of polystyrene and poly(methyl methacrylate) were purchased from Polymer Laboratories and Phase Separations Ltd. (U.K.) and Polymer Standards Service (Germany). A monodisperse block copolymer of styrene and methyl methacrylate, containing mass fraction 0.487 of styrene, was also purchased from Polymer Laboratories. Mass-average molar masses M_w and polydispersity indices M_w/M_n for all polymers are given in Table 1. Cyclohexane and cyclohexanol of mass fraction purity > 0.999 were purchased from Aldrich and used as solvents without further purification.

Sample Preparation. Polymer samples were prepared in situ (i.e., inside the sample cells). The turbidimeter cell block was first assembled and then weighed to ± 1 mg. Having calculated the masses of polymer and solvent desired, a preweighted quantity of polymer was carefully added to the first cell. Next, with the cell block still on the balance, the required amount of solvent was introduced, the precise amount determined gravimetrically, and the cell immediately sealed. This process was repeated until all five cells were filled. The cell loading was chosen such that the resulting solution occupied approximately 60 % of the available volume. This ensured that the optical path always passed through the liquid while avoiding the possibility of cell rupture on heating.

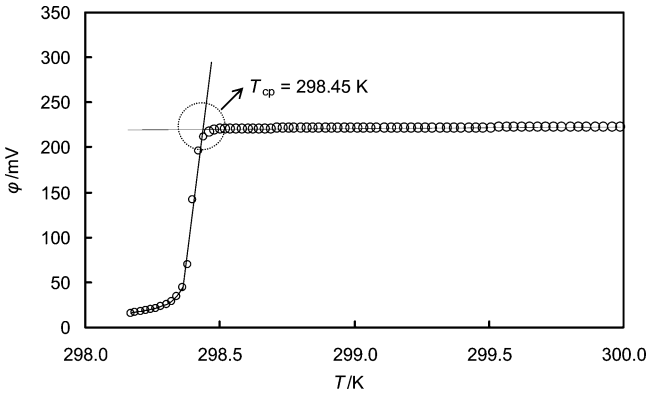

Figure 2. Photodetector output voltage φ as a function of sample temperature T for PS 286 in cyclohexane with $w = 0.048$ showing the location of the cloud-point at $T = 298.45$ K.

Experimental Procedure. With the polymer and solvent samples sealed in the turbidimeter, the rest of the apparatus was assembled and left for a few hours during which the polymer underwent swelling and partial dissolution. The motor was then started to promote mixing, and the rocking speed and angle were set manually to suit the viscosity of the solutions. The temperature was then set at what was expected to be a single-phase state: for UCST systems a temperature of 20 to 40 K above the θ temperature was chosen. Stirring was maintained at this temperature for 2 h to ensure homogeneity in the one-phase region. After this time the motor was switched off, and the turbidimeter returned to its rest position. The turbidity was then monitored at constant temperature (typically 1 h) until it was constant. This settling period was required to ensure disentrainment of vapor bubbles from the liquid. A cooling ramp lasting several hours was then programmed during which the experimental data were gathered. All experiments were carried out at the vapor pressure of the system.

Test System. Initial experiments were carried out on the system PS + cyclohexane for which the phase behavior is well-documented.[10] This system exhibits both UCST and LCST behavior. Polydisperse polystyrene of $M_w = 286$ kg·mol^{-1} was used, and a number of polymer solution concentrations were studied. For this molecular weight of the polymer, the results of Saeki et al.[10] show that the UCST should occur at approximately 298 K and the LCST at approximately 498 K. All samples were mixed in situ at $T = 333$ K, where they became transparent, and then were cooled at a controlled rate until phase separation was observed. Figure 2 shows the output of the photodetector as a function of temperature for the cell containing the solution with mass fraction $w = 0.048$. A distinct drop in transmitted light intensity occurred at a temperature of 298.45 K, and this was identified as the cloud-point temperature T_{cp}. The results for all five compositions studied are given in Table 2. In the next test, all cells were loaded with the same concentration, $w = 0.048$, and the lower binodal curve was then measured. In a given cooling run, the results from four cells agreed to within ± 0.2 K, while two different runs with cooling rates of 0.042 and 0.018 K·min^{-1} gave $T_{cp} = 298.6$ K and $T_{cp} = 298.4$ K, respectively, as the mean values from four cells. Unfortunately, the fifth cell leaked, so no results were obtained for that channel. Following these measurements, the same samples were remixed at $T = 373$ K and then ramped upward at a rate of 2.1 K·min^{-1} until the upper binodal curve was

Table 2. Cloud-Point Temperatures T_{cp} for PS + Cyclohexane as a Function of the Mass Fraction w of Polymer[a]

$10^2\,w$	T_{cp}/K (run 1)	T_{cp}/K (run 2)
1.30	297.95	298.70
1.94	299.02	298.95
2.27	299.00	298.38
4.80	298.35	298.45
0.94	297.07	*b*

[a] $M_w = 286$ kg·mol^{-1}. [b] Cell leakage prevented measurement.

Table 3. Cloud-Point Temperatures T_{cp} for PS + Cyclohexane with $w = 0.048$ and $M_w = 286$ kg·mol^{-1} for Various Temperature Ramping Rates $\dot{T}$

$\dot{T}$/(K·min^{-1})	T_{cp}/K (cell 1)	T_{cp}/K (cell 2)	T_{cp}/K (cell 3)	T_{cp}/K (cell 4)
−0.042	298.55	298.45	298.65	298.90
−0.018	298.30	298.20	298.40	298.50
4.0	496.15	493.65	493.65	497.15
2.1	496.15	494.15	494.15	496.15

Table 4. Cloud-Point Temperatures T_{cp} for PS + Cyclohexanol as a Function of the Mass Fraction w of Polymer

$M_w = 4.215$ kg·mol^{-1}		$M_w = 78.8$ kg·mol^{-1}		$M_w = 849$ kg·mol^{-1}	
$10^2\,w$	T_{cp}/K	$10^2\,w$	T_{cp}/K	$10^2\,w$	T_{cp}/K
1.27	300.87	0.70	347.14	0.84	353.29
1.97	304.72	1.11	347.39	1.90	353.50
3.35	310.42	1.93	348.89	3.58	353.34
4.05	312.91	1.95	349.30	3.99	353.20
5.22	315.01	3.34	350.04	5.50	353.27
8.70	321.04	4.13	351.65		
10.05	320.24	4.69	351.80		
12.52	319.39	8.39	351.73		
15.07	318.54	9.63	351.82		
20.26	317.91	12.14	351.95		

crossed. In this case, the cloud-points determined from the four "good" cells spanned a range of 2.0 K with a mean value of 495.2 K. This test was repeated at a ramping rate of 4.0 K·min^{-1} with the same result for the mean cloud temperature and a similar spread between the cells. The results for $w = 0.048$ are summarized in Table 3. We mention that a potentially significant source of experimental error arises for the upper binodal curve because of the rapidly increasing vapor pressure of the solvent. Constant-volume flash calculations suggest that several percent of the solvent may be transferred to the vapor space on heating to $T \approx 495$ K, and this is sufficient alter the liquid-phase composition significantly.

Our test data for PS + cyclohexane are compared with the results reported by Saeki et al.[10] in Figure 3. To make a quantitative comparison, interpolations with respect to both molar mass and composition are required. On the lower binodal curve, we interpolate to $w = 0.03$ with a quadratic polynomial and find $T_{cp} = 299.0$ K for our PS sample with $M_w = 286$ kg·mol^{-1}. Saeki et al. include results for $M_w =$ (200 and 400) kg·mol^{-1}, and linear interpolation to $M_w = 286$ kg·mol^{-1} gives $T_{cp} = 298.4$ K at $w = 0.03$. The uncertainty associated with these interpolations is difficult to estimate precisely but certainly does not exceed 0.5 K. We conclude that there is excellent agreement between the test results and those of Saeki et al.

Results and Discussion

The three polymers PS, PMMA, and PS-*b*-MMA were studied with cyclohexanol as a common solvent. In each case, initial rapid temperatures ramps confirmed that only a lower binodal curve with a UCST existed in the accessible temperature range.

PS + Cyclohexanol. The cloud-point curves of three different molar masses of polystyrene in cyclohexanol were measured

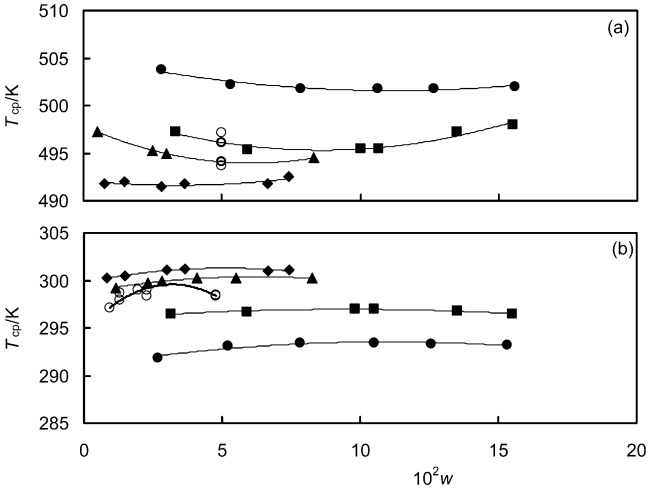

Figure 3. Cloud curves of PS + cyclohexane: panel a, LCST branch; panel b, UCST branch. This work: ○, PS 286. Saeki et al.[9]: ●, PS 97; ■, PS 200; ▲, PS 400; ◆, PS 680. Curves are quadratic polynomials.

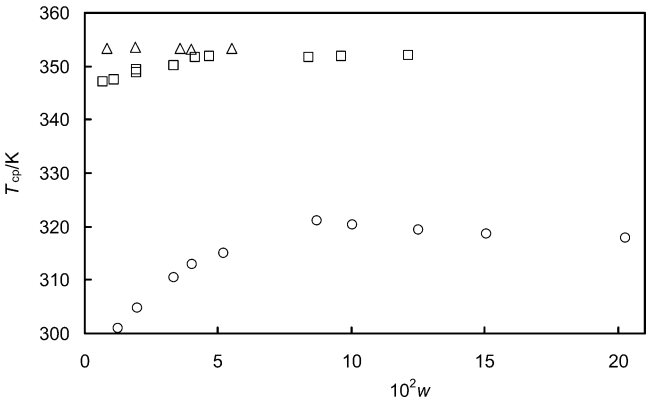

Figure 4. Cloud curves of PS + cyclohexanol: ○, PS 4; □, PS 79; △, PS 850.

for $w \leq 0.20$, and the results are summarized in Table 4 and in Figure 4. The repeatability of T_{cp} varied between ± 0.2 K and ± 0.8 K. The upper critical solution temperatures increase with increasing molar mass and appear to approach a limiting value close to the reported θ temperature of 356.15 K.[21] In common with other polymer solutions, the cloud-point curves are very flat.

The phase behavior of PS + cyclohexanol can be compared to that of PS + cyclohexane. Two observations can be made: first, the presence of the OH group eliminates an upper binodal curve from the accessible temperature range; second, the miscibility gap for a given molar mass of PS is narrower in cyclohexanol than in cyclohexane. These results are consistent with the results of arguments based on the solubility parameters of the polymer and solvents. The solubility parameter S is defined as the square root of the cohesive energy density, and it takes values of 18.1 MPa$^{1/2}$ for PS, 16.8 MPa$^{1/2}$ for cyclohexanol, and 23.3 MPa$^{1/2}$ for cyclohexane.[22] Since S for PS is closer to that of cyclohexanol than it is to that of cyclohexane, it is to be expected that PS will be more miscible in the alcohol.

PMMA + Cyclohexanol. Three different molar masses of the polymer were studied for $w \leq 0.17$, and the results are given in Table 5 and in Figure 5. The repeatability of T_{cp} varied between ± 0.1 K and ± 0.6 K. Concentrations in excess of $w = 0.17$ were not studied as the "flaky" nature of the polymer made it difficult to put larger amounts into the cells. As observed for the PS + cyclohexanol systems, the cloud-point curves

Table 5. Cloud-Point Temperatures T_{cp} for PMMA + Cyclohexanol as a Function of the Mass Fraction w of Polymer

$M_w = 68.0$ kg·mol^{-1}		$M_w = 280$ kg·mol^{-1}		$M_w = 992.2$ kg·mol^{-1}	
$10^2 w$	T_{cp}/K	$10^2 w$	T_{cp}/K	$10^2 w$	T_{cp}/K
0.14	344.48	0.14	347.39	0.15	348.36
0.45	344.89	0.26	347.42	0.44	350.05
0.73	345.39	0.68	348.72	1.00	349.38
1.06	344.02	1.38	349.02	1.03	350.58
1.70	345.12	2.34	349.06	1.90	350.40
2.11	345.20	5.23	350.85	4.75	350.51
5.11	346.15	7.88	350.12	8.60	349.42
9.82	346.69	10.05	350.25	9.68	350.24
12.98	346.30	11.02	350.38	14.75	350.18
13.29	346.59	11.63	350.73	16.90	349.49

Table 6. Cloud-Point Temperatures T_{cp} for PS-*b*-MMA 59 + Cyclohexanol as a Function of the Mass Fraction w of Polymer

$M_w = 58.5$ kg·mol^{-1}		$M_w = 58.5$ kg·mol^{-1}	
$10^2 w$	T_{cp}/K	$10^2 w$	T_{cp}/K
0.15	340.74	9.41	345.61
0.62	346.65	11.79	345.45
1.04	347.14	15.89	345.73
4.17	345.68	16.39	344.80
6.02	345.41	18.30	345.15

appear to be very flat, and cloud-point temperatures increase with increasing M_w. However, this increase is much smaller than we observe for the PS solutions. The flatness of the curves makes it difficult to locate the critical solution point precisely on the composition axis; nevertheless, the UCST itself appears to approach a limiting value slightly above 350 K as M_w becomes very large. This is in agreement with the θ temperature of 351.95 K reported by Kotaka et al.[21].

PS-b-MMA + Cyclohexanol. Finally, the cloud curve of a nearly 50:50 block copolymer was measured. Only one molecular weight was available, and the results for $w \leq 0.18$ are given in Table 6 and in Figure 6. The repeatability of T_{cp} varied between $\pm$ 0.1 K and $\pm$ 0.6 K. We observe binodal temperatures $T_{cp} \leq 347$ K, which seem reasonable in comparison with the reported theta temperature for this system of 353.95 K.[21] In Figure 5, we also plot the curves for PS 79 and PMMA 68. Unfortunately, since the molar masses are not exactly the same, direct comparison is not possible but it seems likely that had the pure polymers had the same molar mass as the copolymer then the cloud-point curve of the copolymer would lie between those of the pure polymers.

Conclusions

A simple thermo-optical apparatus was constructed for the detection of liquid−liquid phase separation, and it proved to be useful in the determination of cloud curves in polymer solutions. Pressures up to about 3 MPa and temperatures in the range 293 to 523 K can be accessed. Solutions with mass fractions of polymer up to 0.25 were studied, and less than 1 mL of each solution was required, making the method particularly convenient for the study of high-value or scarce materials. The accuracy of the method is difficult to determine precisely. However, in the light of the results for the test system and the apparent scatter in some of the other measurements, we estimate that the accuracy of the cloud temperatures in the present work is approximately $\pm$ 0.5 K. We expect that this could be improved significantly in the future. For example, the sealing arrangement used in the present work was not optimal, and some unreported measurements were affected by leakage.

The phase behavior of solutions of PS, PMMA, and PS-*b*-MMA was successfully measured, and the results are consistent with θ temperatures obtained from the literature. All three systems exhibited only UCST behavior in the temperature and pressure range studied. As expected, the UCSTs increased with increasing M_w, but this increase was much more marked for PS than it was for PMMA. In addition all cloud-point curves were very flat, especially those for PMMA and the copolymer solutions, suggesting that the polymer-rich phase may contain very little solvent. Finally the cloud curve of the block copolymer appears to lie between those of the two corresponding pure polymers if the molar masses are the same.

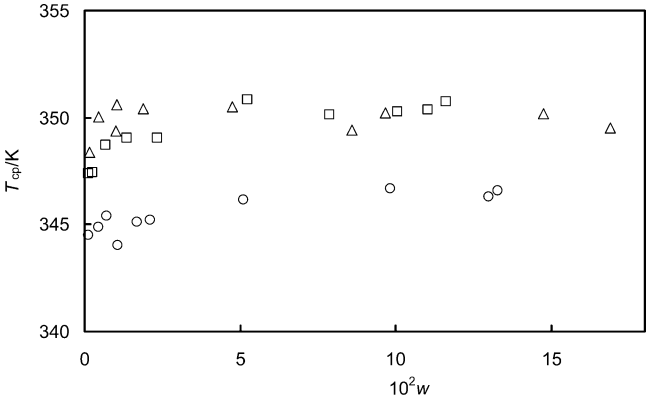

Figure 5. Cloud curves of PMMA + cyclohexanol: ○, PMMA 68; □, PMMA 280; △, PMMA 992.

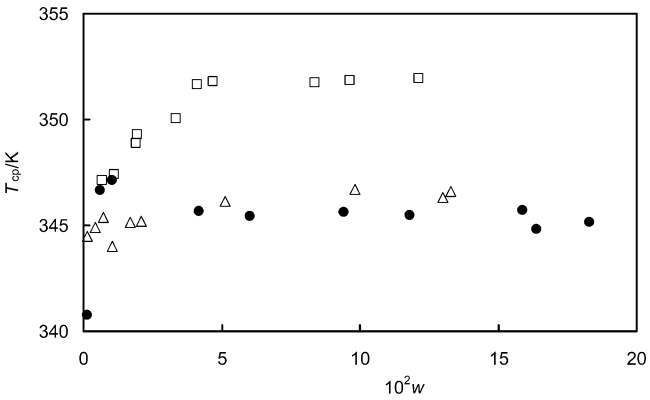

Figure 6. Cloud curves of polymer + cyclohexanol: ●, PS-*b*-MMA 59; □, PS 79; △, PMMA 68.

Acknowledgment

We are grateful to Dr. Andrew Burgess for many stimulating discussions during this project.

Literature Cited

(1) García Sakai, V. Polymer solution thermodynamics. Ph.D. Thesis, University of London, 2002.
(2) Hao, W.; Elbro, H. S.; Alessi, P. *Polymer Solution Data Collection. Part 3: Liquid−Liquid Equilibrium*; Chemistry Data Series, Vol. XIV; DECHEMA: Frankfurt, Germany, 1992.
(3) High, M. S.; Danner, R. P. *Handbook of Polymer Solution Thermodynamics*; DIPPR, AIChE: New York, 1993.
(4) Wolfarth, C. *Vapour−Liquid Equilibrium Data of Binary Polymer Solutions*; Elsevier: Amsterdam, 1994.
(5) Koak, N.; Visser, R. M.; de Loos, Th. W. High-pressure phase behaviour of the systems polyethylene + ethylene and polybutene + 1-butene. *Fluid Phase Equilib.* **1999**, 160.
(6) Schultz, A. R.; Flory, P. J. Phase behaviour in polymer−solvent systems. *J. Am. Chem. Soc.* **1952**, *74*, 4.
(7) Pruessner, M. D.; Retzer, M. E.; Greer, S. C. Phase separation curves of poly(α-methylstyrene) in methylcyclohexane. *J. Chem. Eng. Data* **1999**, *44*, 1999.
(8) Hamada, F.; Fujisawa, K.; Nakajima, A. Lower critical solution temperature in linear polyethylene−*n*-alkane systems. *Polym. J.* **1973**, *4*, 316.

(9) Liddell, A. H.; Swinton, F. L. Thermodynamic properties of some polymer solutions at elevated temperatures. *Discuss. Faraday Soc.* **1970**, *49*, 115.
(10) Saeki, S.; Kuwahara, N.; Konno, M.; Kaneko, N. Upper and lower critical solution temperatures in polystyrene solutions. *Macromolecules* **1973**, *6*, 246.
(11) Saeki, S.; Konno, M.; Kuwahara, N.; Nakata, M.; Kaneko, N. Upper and lower critical solution temperatures in polymer solutions. III. Temperature dependence of the χ_1 parameter. *Macromolecules* **1974**, *7*, 521.
(12) Konno, M.; Saeki, S.; Kuwahara, N.; Kanata, M.; Kaneko, N. Upper and lower critical solution temperatures in polystyrene solutions. IV. Role of configurational heat capacity. *Macromolecules* **1975**, *8*, 799.
(13) Cowie, J. M. G.; Maconnachie, A.; Ranson, R. J. Phase equilibria in cellulose−acetone solutions. The effect of the degree of substitution and molecular weight on upper and lower critical solution temperatures. *Macromolecules* **1971**, *4*, 57.
(14) Hino, T.; Song, Y.; Prausnitz, J. M. Liquid−liquid equilibria and theta temperatures in binary solvent−copolymer solutions from a perturbed hard-sphere equation of state. *J. Polym. Sci.: Polym. Phys.* **1996**, *34*, 1977.
(15) Siow, K. S.; Delmas, G.; Patterson, D. Cloud point curves in polymer solutions with adjacent upper and lower critical solution temperatures. *Macromolecules* **1972**, *5*, 29.
(16) Kyoumen, M.; Baba, Y.; Kagemoto, A.; Beatty, C. L. Determinations of consolute temperature of poly[styrene-*ran*-(butyl methacrylate)] solutions by simultaneous measurement of differential thermal-analysis and laser transmittance. *Macromolecules* **1990**, *23*, 1085.
(17) Meilchen, M. A.; Hasch, B. M.; McHugh, M. A. Effect of copolymer composition on the phase behaviour of mixtures of poly(ethylene-*co*-methyl acrylate) with propane and chlorodifluoromethane. *Macromolecules* **1991**, *24*, 4874.
(18) Szydlowski, J.; van Hook, A. W. Studies of liquid−liquid demixing of polystyrene solutions using dynamic light scattering. Nucleation and droplet growth from dilute solution. *Macromolecules* **1998**, *31*, 3255.
(19) van Hook, W. A.; Wilczura, H.; Rebelo, L. P. N. Dynamic light scattering of polymer/solvent solutions under pressure. Near-critical demixing ($0.1 < p/\text{MPa} < 200$) for polystyrene/cyclohexane and polystyrene/methyl cyclohexane, *Macromolecules* **1999**, *32*, 7299.
(20) Bae, Y. C.; Lambert, S. M.; Soane; D. S.; Prausnitz, J. M. Cloud-point curves of polymer solutions from thermo-optic measurements. *Macromolecules* **1991**, *24*, 4403.
(21) Kotaka, T.; Tanaka, T.; Ohnuma, H.; Murakami, Y.; Inagaki, H. Dilute solution properties of styrene−methyl methacrylate copolymers with different architecture. *Polym. J.* **1970**, *1*, 245.
(22) Brandrup, J.; Immergut, E. H. *Polymer Handbook*; Wiley-Interscience: New York, 1975.

Received for review November 18, 2005. Accepted January 3, 2006. We are pleased to acknowledge financial support from the Strategic Research Fund of ICI plc.

JE0504865